Observed and projected changes in extreme drought and wet-prone regions over India under CMIP5 RCP8.5 using a new vulnerability index

Pravat Jena
IIT Mandi: Indian Institute of Technology Mandi
sarita azad (sarita@iitmandi.ac.in)
IIT Mandi

Research Article

Keywords: Extreme drought event, Extreme wet event, SPI, Vulnerability index, CMIP5

Posted Date: March 4th, 2021

DOI: https://doi.org/10.21203/rs.3.rs-286354/v1

Observed and projected changes in extreme drought and wet-prone regions over India under CMIP5 RCP8.5 using a new vulnerability index.

Pravat Jena[1], Sarita Azad[2*]

[1, 2]: School of basic sciences, Indian Institute of Technology Mandi, H.P-175005, India

*Corresponding author[2]: Sarita Azad

Email: sarita@iitmandi.ac.in

Abstract

Past versions of vulnerability index have shown ability to detect susceptible region by assessing socio-economic parameters at local scales. However, due to variability of these vulnerability index respect to socio-economic parameters, cann't be utilized to predict the susceptibility region. The present endeavor aims to develops a new vulnerable index which identify and predict the spatio-temporal imprint of extreme drought and wet events at various scales in India by analyzing monthly observed and Coupled Model Inter-Comparison Phase 5 (CMIP5) rainfall data at spatial scale $1^o \times 1^o$ of time period pertaining to 1901-2100. New vulnerability index is proposed by consolidating the outcomes of Standard Precipitation Index (SPI) at different time scales such as 3- and 12-month and along with weights of individual grids. The weights of individual grid is calculated through the occurrence of extreme drought and wet events in the recent past which is to include a climate change factor in the proposed index. Based on the spatial distribution of high index values, the expected vulnerable regions concerning extreme drought events will be in Northeast, Northeast Central, East Coast, West, Northwest, Northcentral, and some grids in South

part of India. Similarly, vulnerable regions concerning extreme wet events are likely to be in the Northeast, West Coast, East Coast, and some grids in the Peninsular region.

Further, a conceptual model is presented to quantify the severity of extreme events. The analyses reveal that on the CMIP5 model data, it is obtained that 2024, 2026-27, 2035, 2036-37, 2043-44, 2059-60, 2094 are likely to be the most prominent drought years in all-India monsoon rainfall and their impact will persist for a longer time. Similarly, the most prominent wet events are predicted to be 2076, 2079-80, 2085, 2090, 2092, and 2099.

Keywords: Extreme drought event, Extreme wet event, SPI, Vulnerability index, CMIP5.

1. Introduction

Precipitation is one of the critical components of the hydrological cycle that has been affected by climate change (Fowler and Hennessy 1995; Xie et al. 2010). Consequently, it has witnessed more frequent extreme events (wet/droughts) (Zhang et al. 2008). Extreme weather events are a common feature, which depends on either deficit or excess of rainfall over a region, and their co-existence poses a potent threat. The formation of droughts is slow, and it takes a long time to evolve, months to years; therefore, exceptional events are hard to be predicted. However, the floods are the immediate response of disturbed weather conditions and are easily quantifiable. As a result, occurrences of both the events cause significant damages mainly to agriculture and loss of livelihood (Vasiliades et al. 2011; Narasimhan and Srinivasan 2005). More than one-third of the available landmasses in India are of semi-arid and arid tropical types, which are vulnerable to frequent droughts and desertification (Nagarajan 2003). Hence, it is necessary to understand the

formation of drought over different landmasses of India with changes in the climate at regional scales.

Many parts of the world including India have experienced an increase in the frequency of occurrence of flood and drought events in the recent past (Mallya et al. 2016; Meehl et al. 2005; Mishra and Singh 2010; Parthasarathy et al. 1994; Peters et al. 2005; Preethi et al. 2019; Rajeevan et al. 2008; Veijalainen and Vehvilainen 2008). Standard Precipitation Index (SPI) (Mckee et al. 1993) is the most famous index available for detection of drought and wet events, as recommended by the World Meteorological Organization (WMO) (Hayes et al. 1999; Svoboda and Fuchs 2016). The SPI has several advantages due to its simplicity and temporal flexibility, which allow its application for water resources at different time scales. For example, the SPI index is generally calculated for the selected periods, i.e. 3, 6, 12, and 24 months. The SPI at time scales 3-and 6-month describe drought/wet events affecting agricultural practices as these time scales can conclusively indicate the soil moisture conditions of vegetation for the growing season (Tsakiris & Vangelis 2004; Jena et al. 2020). Further, the SPI values at the longer time scales such as 12- and 24-month are pertinent for water resources management purposes (Edwards and McKee 1997; Bonaccorso et al. 2003).

According to the Intergovernmental Panel on Climate Change (IPCC), vulnerability defines as "the degree of susceptibility to damage". It is the result of "diverse historical, social, economic, political, cultural, institutional, natural resource, and environmental conditions and processes" (Lavell et al. 2012). The selection of vulnerability indicators or variables varies based on local study context and purposes. Several vulnerability indices are available in the literature, in which some are derived from SPI, and others are proposed independently of SPI along with the local drought indicator. For example, Yang et al. (2012) have proposed a drought vulnerability

index (DVI) using the trend test over ten drought indicators. These indicators were taken from three different sectors, such as water resources, precipitation patterns, and social aspects, and trend tests were applied to score DVI. However, the analysis is a constraint to the indicators, and it applies only to the river basin. Murthy et al. (2015) have developed a composite index, known to be agricultural drought vulnerability index (ADVI) to measure the agriculture vulnerability to drought at a local scale in the Andhra Pradesh state of India by analyzing 22 indicators over spatial coverage. The variance approach generates the weights of each input indicator to quantify the severity of drought to agriculture. Although ADVI can classify (vulnerable and non-vulnerable) the region, it is restricted to local scale as the input parameters are susceptible to the areas because of the complexity in geographical structure and weather pattern. Further, some studies have reported vulnerability assessment associated with the climate changes in water resources, agricultural sector, socio-economic indicators such as land use, technology, and infrastructure (Metzger et al. 2005; Eakin and Conley 2002; Brooks et al. 2005).

Manikandan and Tamilmani (2013) have proposed a DVI, which is derived index from SPI considering the parameters such as its drought spatial extends, frequency (drought occurrence), and severity (drought categories that are, moderate to extreme drought). Another DVI developed by Kim et al. (2015) and Dabanli (2018) considered socio-economic parameters such as Irrigated Land (IL), Total Agricultural Land (TAL), Population Density (PD), and Municipal Water (MW). Similarly, different sets of drought parameters have been taken into consideration in a study conducted by Kar et al. (2018) to identify the vulnerable regions through assigning appropriate weights parameters. The Standardized Drought Vulnerability Index (SDVI) is an index developed by Oikonomou et al. (2019) which incorporates precipitation patterns, the supply and demand trends, and the socio-economic background to drought vulnerability. In this framework, in-situ and

satellite data are utilized to minimize the lack of drought-related information. The temporally varying signs such as SPI, surface water drought index (SWDI), and groundwater drought index (GDI) and spatial information of the indicators have been integrated to measure the vulnerability to droughts over Bundelkhand in central India (Thomas et al. 2016).

The General circulation models (GCMs) constitute essential tools for assessing probable impacts of climate change over various representative concentration of pathways (RCPs). The coupled model intercomparison project five (CMIP5), a framework for analyzing and quantifying the results of the Atmosphere-Ocean Coupled General Circulation Model (AOCGCM) (Taylor et al. 2011). These CMIP5 projections are based on updated global greenhouse gas emission scenarios represented as a radioactive concentration of pathways (RCPs). Many studies have employed CMIP5 models to investigate the evolution of past and future droughts and predicting the severity of future droughts (Cook et al. 2015; Sheffield and Wood 2008; Taylor et al. 2013; Zhao and Dai 2015; Swann et al. 2016; Orlowsky and Seneviratne 2013). In the context of India, a recent study by Preethi et al. (2019) assessed the variability of drought and wet events using CMIP5 models and reported the frequent occurrence of droughts during the near and mid future (2010-2059). A study carried by Ojha et al. (2013) considering 17 GCMs has assessed the severe droughts and wet events in the future. The study has reported an increasing trend in the frequencies of droughts and wet events. It is shown that drought events are expected to increase in the West Central, Peninsular, and central Northeast regions of India in the future. In contrast, the northern parts of India and coastal areas are likely to experience a maximum increase in the frequency of wet events.

Numerous factors influence drought vulnerability, which are directly pertinent to the local studies (UNDP 2004). Several studies have been performed to assess the vulnerability of a region

112 related to the effect of climate changes on meteorological parameters, water resources, and
113 agricultural sectors (Eakin and Conley 2002; Brooks et al. 2005; Metzger et al. 2005). The present
114 study proposes two conceptual models to quantify the severity of extreme drought and wet events
115 and to identify the regions which are vulnerable to such kind of events. For the identification of
116 vulnerable regions, the proposed model uses the SPI outcomes such as frequency, prolonged
117 duration, and magnitude, which reflects the impacts of meteorological extremes at the local scale.
118 In addition, the weight of the grid, which takes into account the pre and post-global warming effect
119 of occurring the meteorological extremes at a local scale is given consideration. For example,
120 suppose two grids experience the same number of extreme events, but a grid which experience
121 such events in the early part of the nineteenth century is less weighted as compared to the one in
122 the latter part of the century. Further, the present study employs CMIP5 projection data to assess
123 the changes in the vulnerable regions in the future. In this framework, firstly observed data is used
124 to identify the vulnerable region and validated through literature, and further, the index is
125 employed on CMIP5 projection datasets.

126 **2. Data, study area, and methodology**

127 **2.1 Data and study area**

128 Observed gridded rainfall data of spatial resolution $1^o \times 1^o$ for the period 1901-2014 is
129 obtained from the open web repository of Climate Research Unit (CRU), UK
130 http://www.cru.uea.ac.uk (Harris et al. 2014). The spatial domain for the analysis comprised of
131 354 grids is chosen in the range of latitude $8^o4' - 37^o5'$ and longitude $68^o5' - 97^o5'$ covering
132 the Indian region. As mentioned in Harris et al. (2014), this precipitation dataset has undergone a
133 quality check by the CRU. Further, it has been compared with other observation-based datasets;
134 namely, Global Precipitation Climatology Center (GPCC), University of Delaware (UDEL),

climate research temperature TEM data (CRUTEM) at a global scale (Becker et al. 2013; Willmott and Matsuura 2001; Jones et al. 2012). And also it has been compared at a regional scale (Shi et al. 2017; Reeves et al. 2017; Thorne et al. 2016) to demonstrate the robustness of this dataset. In the Indian context, Rao et al. (2014) have given preference to CRU data due to its accuracy in comparison to the other datasets such as National Data Centre (NDC), India, and Indian Meteorological Department (IMD). Further, Robertson et al. (2013) have performed a comparative analysis between CRU and IMD data in northern India from 1982 to 2005 and found a reasonable degree of closeness between the two datasets.

Further, the present work utilizes historical and projection simulations of CMIP5 model (Taylor et al. 2012) spanning over the period 1901-2005 and 2006-2100, respectively obtained from the website of Earth System Grid Federation (ESGF) (https://esgf-node.llnl.gov/search/cmip5/). As mentioned in Taylor et al. (2012) CMIP5 datasets are available at different RCPs scenarios, namely 2.6, 4.5, 6.0, and 8.5, and designated based on the concentration of greenhouse gases and the possible range of radiative forcing values towards the 2100. In RCP 2.6 and 4.5, emissions continue to rise till 2030 and 2040, respectively and its trend declines towards 2100. Similarly, in RCP 6.0 emissions continue to rise till 2060, and it stabilizes towards 2100, while in RCP8.5, the emissions continue to increase throughout the 21st century. In view of importance of RCP8.5, we have utilized this data set in the present work. The CMIP5 models outputs were developed at different climate centers over the globe with various horizontal resolutions. Therefore, these models are rescaled to the spatial resolution of observations using a bilinear interpolation technique. The bilinear interpolation has been used for rescaling the climate variable such as rainfall data in various climate studies over the globe (Diffenbaugh and Giorgi 2012; Geil et al. 2013; Koirala et al. 2014).

158 Further, gridded data is used to calculate the all-India rainfall by taking the area-weighted
159 average over all grids using a standard weighted matrix (Rajeevan et al. 2006) provided by the
160 IMD.

161 The observed data is partitioned into three parts such as 1901-1937 (first time-domain
162 (FTD)), 1938-1976 (second time-domain (STD)), and 1977-2014 (third time-domain (TTD)). The
163 rationale of dividing the data into three parts is to identify spatio-temporal shift of rainfall extremes
164 over time and to preserve stationarity in data. Further, the statistical test, Dickey-Fuller test is
165 employed to check stationarity over each segment of the data. The null hypothesis of the Dickey-
166 Fuller (ADF test) (Dickey and Fuller, 1981) is rejected (p-value < 0.01), which indicates that data
167 maintain stationarity concerning the statistical properties.

168 **2.2 Ensemble of CMIP5 Models**

169 An assessment of the performance of climate models in simulating the variability in
170 drought and wet events for the time of 1901–2005 using CMIP5 (Taylor et al. 2012) is presented.
171 Historical simulations from 12 CMIP5 models, which represent Indian summer monsoon rainfall
172 (Jena et al. 2015, 2016; Jena and Azad 2019; Azad and Rajeevan 2016) is compared with the
173 corresponding observations to obtain an assessment of the models' performance, which is
174 mentioned in Table 1. Further, an ensemble of these selected models is formed by implementing
175 Shannon's entropy method. It assigns weights to each model based on the performance in
176 simulating observed climatology such as JJAS, and annual rainfall (in mm). Using these
177 climatologies, the statistics such as coefficient variation (CV), root mean square error, and
178 Correlation of coefficient (CC) are computed for each CMIP5 model dataset. The obtained
179 statistics form a matrix of the dimension (12 X 6), which is known to be decision matrix. The detail
180 procedure as follows:

Step 1: Shannon's entropy (Shannon 1948) is a method to find the desired weights for the given criteria which can be assessed as

$$e_k = -\frac{1}{ln(n)}\sum_{i=1}^{n} z_{ik}\, ln(z_{ik}) \quad (1)$$

$$d_k = 1 - e_k \quad (2)$$

where, z_{ik} is the normalized form of the decision matrix, n is the number of models and e_k is the Shannon entropy, which gives the information of the individual model's weightage used in the analysis.

Step 2: The weights can be written as

$$w_k = \frac{d_k}{\sum_{k=1}^{m} d_k} \quad (3)$$

Step 3: An ensemble of data is formed by

$$data = \sum_{i=1}^{n}(m_i * w_i) \quad (4)$$

where, n is the number of models, m_i is the CMIP5 model data, and w_i is the weight of the corresponding models.

The ensemble model data is compared with the observations as well as individual models' climatology of Indian monsoon rainfall. The results are shown in Table 2 and reveal that an ensemble model performs better than individual models in simulating observed climatology. For example, the model GFDL-ESM2G shows a 2% relative error (RE) in simulating the annual amount of rainfall, which is less than other models as well as the ensemble model. However, this model has a high value of RE (>=27%), while simulating June-September (JJAS) climatology. A similar observation is also noticed in other selected models. So, it is concluded that there is no

unique model whose performance in simulating the climatology of JJAS and annual rainfall is outstanding. However, it is observed that an ensemble model has less RE (5% for annual rainfall, 15% for JJAS rainfall) which is relatively less than other individual models in simulating both observed climatology. Therefore, an ensemble model is chosen for the historical and projection analysis.

2.2 Methodology

2.2.1 SPI

SPI is utilized to investigate the spatial, temporal extent, and severity of droughts occurrence over the region. This index is defined as the difference between the rainfall at a given instance and the long-term mean divided by the standard deviation in the specified time domain. However, this method cannot be applied directly as the precipitation follows skewed distribution for the accumulation period of 12 months or less (Mckee et al. 1993). This disadvantage can be overcome by applying simple transformation functions which converts the skewed distribution into a normal distribution.

Normally, the SPI index is calculated for the selected periods, i.e. 3, 6, 12, and 24 months. The time scale 3-and 6-month give the information about the short-term drought/wet, whereas 12- and 24- month provide long term drought/wet. It is mentioned that the gamma distribution fit the climatological precipitation data well, therefore, the monthly precipitation time series for j^{th} time scale is modeled using gamma distribution (Thom 1958). In the present study, various distributions are fitted to rainfall data and it reveals that gamma distribution closely fits (See Appendix). The probability density function of the gamma distribution is defined by:

$$g(x) = \frac{1}{\beta^{\alpha}\gamma(\alpha)} x^{\alpha-1} e^{-\frac{x}{\beta}} \text{ for } x > 0 \quad (5)$$

where $\alpha > 0$ is a shape parameter, $\beta > 0$ is a scale parameter, and $x > 0$ is the amount of precipitation. $\gamma(\alpha)$ is the gamma function which is defined as:

$$\gamma(\alpha) = \int_0^\infty y^{\alpha-1} e^{-y}\, dy \tag{6}$$

The mathematical form of the cumulative probability function of Gamma distribution is given by:

$$G = \int_0^x g(x)dx = \frac{1}{\beta^\alpha \gamma(\alpha)} \int_0^x x^{\alpha-1} e^{\frac{-x}{\beta}} dx \tag{7}$$

Since the gamma distribution is undefined for $x = 0$, the cumulative distribution function for gamma distribution which accounts zero value in the data is further modified as:

$$H(x) = q + (1 - q)G(x) \tag{8}$$

where q represents the probability of zero rainfall over the period $1901 - 2014$.

The algorithm of SPI is implemented on all-India and gridded monthly rainfall data for the period 1901-2014 at different time scales, representing short to long term rainfall events. Using the classification scheme mentioned in McKee et al. (1993), rainfall events are categorized into moderate, severe, and extreme events (both drought and wet).

2.2.2 Severity assessment of extreme drought and wet years

The implementation of SPI provides positive and negative indices, through which extreme drought and wet events are extracted by utilizing the threshold as mentioned in Mckee et al. (1993) and Svoboda and Fuchs (2016). The severity of an extreme drought/wet event is quantified through its magnitude, duration, or how long it persists over time. To understand the impact of extreme (drought and wet) events, a conceptual model is proposed, which is described in Fig. 1. The model calculates the severity index, which is defined as a function of duration and magnitude of the extreme events. The high values of severity index indicate the potential impact of extreme events

and vice versa. Suppose, an extreme event occurred with high magnitude and it persists over a small period, then it is likely to have less potential impact. Whereas, an event with a low magnitude which continues over a long period is likely to have a high impact. The conceptual model takes care of these two aspects and is defined as:

$$S = M \times W \tag{9}$$

where M and W are the magnitude and weight of the corresponding events. The weight of the extreme events is assigned according to the duration of the events. The event with prolonged duration is assigned more weights and vice versa. The magnitude of either event is calculated as:

Step 1: The implementation of SPI algorithm at a given time scale on rainfall time series ($m \times 1$), where m represents the total number of months, it results in SPI index, named as $Index_{m\times 1}$. Transform this matrix to $S_{n\times p}$, where $n = \frac{m}{12} = 114$ and p represents number of years and months, respectively. In this study, extreme rainfall events are considered and the value of threshold (thr) is ± 2 for extreme wet and drought, respectively.

Step 2: Extract the extreme wet years, $d = \{y_1, y_2, y_3, \dots\}$ in which $y_i = \{S_{i,j} \geq thr | i = 1,2,..,n \text{ and } j = 1,2,..,p\}$. Similarly for the extreme drought year, $y_i = \{S_{i,j} \leq thr \,| i = 1,2,..,n \text{ and } j = 1,2,..,p\}$.

Step 3: For i^{th} extreme wet year, find the j^{th} month which exceeds the thr. Then wet magnitude event is obtained as:

$$M_i = \sum_{t=j}^{k}\{S_{i,t} > 0 |\, y_i \text{ is an extreme wet year}\} \tag{10}$$

Similarly, the magnitude of each extreme drought event calculated as:

$$M_i = \sum_{t=j}^{k}\{S_{i,t} < 0 |\, y_i \text{ is an extreme drought year}\} \tag{11}$$

It is a cumulative sum of the magnitude $(k-j)$ positive/negative index value of ith extreme wet/drought year when it encounters with negative/positive index value ($S_{i,k+1} <> 0$).

Then the weight is obtained as:

The weight (W) of extreme wet year is calculated according to the number of months having positive index value after the j^{th} month. For example, if in an i^{th} extreme wet year, five months are having positive index value after j^{th} month, the weight of i^{th} year would be five. Similarly, the weight for extreme drought is obtained.

Further, the values of S is normalized as, $I = \frac{|S|}{max(|S|)}$ to compare at a common scale.

2.2.3 Vulnerability index of rainfall extremes

Generally, the vulnerability is a relative measure among regions/grids concerning rainfall extremes, and it indicates the degree of susceptible to damage (harm) due to the occurrence of an event (Smit et al. 1999). In the present study vulnerable index is defined as a function of frequency, prolonged duration, magnitude, and temporal shift of extreme events over a region. These variables act as distinct indicators of severity concerning drought and wet conditions for a given period. To quantify the vulnerability of a region, a conceptual model is proposed and described in Fig. 2 and its mathematical expressions are described in the equation form, which is stated as:

$$I = P \times WD \times Z \tag{12}$$

where,
$$P = \frac{\sum_{j=1}^{q} D_j}{m} \tag{13}$$

m is the total number of months, D_j represents dry and wet months. Here, dry and wet months are defined according to SPI values negative and positive of the corresponding months respectively

and q is the total number months having SPI value is negative or positive. The term P represents the average number of dry/wet months over the period. Further, P value is calculated over the pre and post era of global warming and accordingly assigns weight to the grids.For example, suppose the grid experienced average dry/wet months equally in pre and post era of global warming, which indicates the grids have less influenced by climate change and hence is assigned less weight. On the other hand, a grid with more average dry/wet months in the post era compared to the pre era of global warming is assigned a relatively higher weight.

The term WD is defined as:

$$WD = \frac{\sum_{j=1}^{n}(d_j)}{(m/12)} \times \frac{\sum_{j=1}^{m} I(Index_j >< thr)}{(m/12)} \quad (14)$$

Here thr represents a threshold for rainfall extremes, d is the extreme event years. The second term of Eq. (14) indicates the frequency of extreme wet and drought over the study period. Two grids may experience the same frequency, so, it is required to assign weight to grids. The assignment of weight to grids is based on the impact of climate change over the region. For example, suppose grid-one and grid-two experienced two extreme droughts such as 1918, 1920; and 1987, 1991, respectively. Here, it may be inferred that there are no changes in the rainfall pattern in the influence of climate change in grid-one, whereas grid-two have adversely influenced by climate change. Therefore, the grid-two is assigned with high weights compared to grid-one and it is calculated by the first term of the Eq. (14).

The term Z is defined below:

$$Z = \frac{\sum_{i=1}^{L_k} M_i \times f_i}{L} \quad (15)$$

where L is the total length of a negative or positive spell of the rainfall events. The negative and positive spell of length L is defined as the L continuous months having $SPI\ index < 0$ and $SPI\ index > 0$, respectively. L_k is the length of spell, where k is the number of spells. For example, in a grid, there are five number of positive spell with each of length of L_1, L_2, L_3, L_4 and L_5. So the total length of the spell is obtained as $L = \sum_{k=1}^{5} L_k$. M_i is the magnitude of dryness/wetness in each spell and f_i is the frequency of rainfall extremes corresponding to the spell. The term f_i add more weightage to the spell, for example, if two grids having the same magnitude and the grid with higher extremes given the more weightage. This situation comes when two or more spells having equal magnitudes, hence the spell with more rainfall extremes is given with the highest weightage. The term Z represents a weighted average drought/wet magnitude in each of the spells. The term Z cumulates the average effect of the droughts and wet magnitude over time. The index I has been constituted in a way to assume larger values for regions that have witnessed more rainfall extremes through fewer and more recent rainfall events. The calculated values of I have been normalized as, $I = \frac{I}{\max(I)}$ and segregated into four intervals based on quartile values.

3. Results and discussion

3.1 All-India observations:

3.1.1 Observed drought and wet events

To preserve stationarity, rainfall data is partitioned into three disjoint sets of equal size 37 years such as 1901-1937, 1938-1976, and 1977-2014. The algorithm of SPI is implemented on each

dataset of monthly rainfall data for the period 1901-2014 at 3- and 12-month scales. It may be noted that the present study focuses only on the extreme rainfall events (extreme drought and wet) and the corresponding years are presented in Table 2 over all-time scales. The results reveal that most of the extreme droughts of 3-month are found to be in 1901-1920 and 1965-2010. A similar result has been reported in Bhalme et al. (1983) and Parthasarathy et al. (1987) that the most of the short-scale droughts were found in 1891-1920 and 1961-1984. Further, a decadal gap (1921-1959) is found in the formation of extreme drought over the time scales of 6-24 months. The large-scale extreme droughts (24-month) occurred between 1960 and 2010.

Similarly, the extreme wet events are extracted and their corresponding years are shown in Table 2. The results reveal that most extreme wet events at a 3 and 12-month scale occurred in 1920-1960, which explains inverse relation between the occurrence of drought and wet events. It may be conferred that in the global warming era (after 1960) the weather events related to temperatures have increased along with the drought events. Similarly, it is noted that before the warming era (before 1960) wet events were more in occurrence along with fewer droughts and temperature events, such as temperature mean change (Narula et al. 2018).

3.1.2 Severity assessment of extreme drought and wet years

The proposed model explained in Section-2.2.2 is employed over the extreme drought and wet years to assess the severity of events. The results of extreme drought events are shown in Fig. 3, in which the subplot of Fig. 3(a) and (b) represent for the time scale of 3-month and 12-month, respectively. At a 3-month scale, the extreme drought years such as 1902, and 1905 have the highest index value which indicates that the influence of these years was persistent for a longer period. The most prominent drought events at 3-month time scale occurred in 1902, 1905, 1908, 1918, and 1920 in the early part of 20^{th} century, and 1966, 1967, 1972, 1987, 1991, 2001, 2002,

2003, and 2009 were designated as major drought events after global warming era. Further considering other time scales, the most prominent years were 1905, 1918, 1964, 1965, 1972, 1987, 2001, and 2002 at a 12-month scale. These extreme droughts have been reported in various literature mentioning the potential impact over diverse fields such as agriculture, water reservoir (Tyalagadi et al. 2015; Samra 2004; Parthasarthy et al. 1987, 1994; Shewale & Kumar 2005). It is well documented that 70% of the Indian region has suffered from the occurrence of extreme drought in 1918, which was designed as first large drought in India followed by second-largest drought in 1987 and 1905, which affected 48% and 37% of the area, respectively (Shewale & Kumar 2005). As mentioned in Samra (2004), the entire region of India has experienced extreme droughts in 2001, 2002, and 2003 which caused many losses in the form of severe damages (US$910,721,000), and many lives were affected (20 deaths and US$90,000,000). It is reported that some of the regions in India (West and Southeast) have experienced extreme droughts in 1987 which further caused loss of lives (approx. 440) and several damages to agriculture; the droughts in 1972 and 1964-65 mainly occurred over the region of central India and Rajasthan (Samra 2004). Further, it is noticed that before the global warming era, there is a decadal gap (1925-1964) of 39 years in which no highly impacted drought has occurred. However, after global warming the decadal gap of occurring highly impacted droughts reduced to 15-, 5- and 9- years.

Similarly, the proposed model is implemented over all the extreme wet years to assess the severity and the corresponding results are presented in Fig. 3, in which the subplot of Fig. 3(c) and (d) represent for 3- and 12-month scales, respectively. Based on the highest index values at a 3-month scale, the most impacted extreme wet years were 1906, 1914, 1916, and 1955 before global warming era, whereas, 1989, 1997, 2005, and 2009 had high impact wet events overtime after the global warming era. Similarly, the most impacted extreme wet events at 12-month were in 1916-

17, and 1955-56 before warming era and 1987, and 2012 after the global warming. Similar results are reported in Preethi et al. (2019), Parthasarathy et al. (1994), Bhalme & Mooley (1980), and Dhar & Nandargi (2003). It is also noticed that the most of wet events occurred after the post era of global warming. Moreover, as mentioned in the IPCC Second Assessment Report (IPCC, 1996) on the projection of Asian/Indian monsoon that the climate models predict more rainfall over these regions in a warmer climate. The warming is associated with the increase in greenhouse gases and might cause an increase in Indian monsoon variability and weaken the strength (IPCC 2001). As mentioned in Bhalme & Mooley (1980), 36% and 28% of the region have experienced extreme wet events in 1916 and 1917, respectively. Further, it is reported that during 1955-56, 1961, and 1975, a large fraction of the area of India such as 27%, 48%, and 31% have experienced major flooding.

3.1.3 Classification of frequency of extremes at gridded level

To visualize the spatial distribution of frequency of the extremes rainfall events at 3- and 12-month scales, the gridded data of resolution $1^{o} \times 1^{o}$ is utilized. As defined in the earlier section, the study period is segregated into three disjoint slices of equal size. For this analysis, the frequency of extreme drought and wet events is calculated in all three time periods. The count of extreme rainfall events over time is known to be frequency and it is obtained as follows:

1. $d_i = Max_{j=1}^{12} S_{i,j}$ or $d_i = Min_{j=1}^{12} S_{i,j}$ for each $i = 1,2,..,n$. Here maximum and minimum numbers represent the highest and lowest SPI value of the specified year, respectively. The dimension of d would be $n \times 1$.
2. The frequency of extreme drought/wet is obtained as

393 $Freq = \sum_{i=1}^{n} I(d_i < \text{or} > thr)$, thr is the threshold value for extreme drought/wet,

394 and I is the indicator function, which is defined as $I(x) = \begin{Bmatrix} 1 | x > 0 \\ 0 | x < 0 \end{Bmatrix}$.

395 Further, the frequency is labeled into 4 classes, including classes 1 to 4, based on their percentile
396 values. The grid having the lower frequency (less than 25th percentile value) of events is considered
397 to be in class 1; frequency lies between 25-49th percentiles is considered to be in class 2; frequency
398 lies in 50-74th percentiles is considered to be in class 3 and frequency greater than 75th percentiles
399 is considered to be in class 4. The results of extreme droughts, which are shown in Fig. 4(a), (b)
400 and (c) reveal that the region East-coast, Northeast-central, Central-peninsula, and North of India
401 at 3-month scale have experienced class 4 frequency of extreme droughts over the FTD, whereas
402 the Northeast and west part of India experienced class 1 and 2 frequencies of extreme droughts.
403 Further, it is seen that there exists a transition from low class to the high-class frequencies of
404 extreme droughts in the Northeast region in STD, which indicates the impact of global warming
405 on monsoonal rainfall over the region. Also, a transition from class 4 to class 3 frequencies of
406 extreme droughts are found over some grids in East, Peninsular, and Northeast central region in
407 STD. In TTD period, it is obtained that South, West, and Peninsular region is experienced with a
408 low class of frequency of extreme droughts, whereas the East and North India experienced class 4
409 frequencies of extreme droughts. It is concluded that the high-class frequencies of extreme
410 droughts are migrated from the South and Peninsula region to the North and East. Similar analyses
411 for the frequency of extreme drought are carried out for the scale of 12-month over three different
412 time domains and the corresponding results are shown in Fig. 4(d), (e) and (f). The results reveal
413 that the class 4 frequencies of extreme droughts are found to cluster in the western part of India,
414 whereas the East and Northeast central of India have experienced class 1 frequencies of extreme
415 droughts in the FTD. In STD, high class of frequency of extreme droughts is distributed non-

uniformly, however, some grids both in the South and Peninsular region experienced class 3 and class 4. In TTD, the class 4 frequencies of extreme droughts are moved to Northcentral and East of India. This result further confirms the previous finding that during the late nineteenth century, India experienced Eastward movement of drought events (Mallya et al. 2016). Moreover, these regions are characterized by no forest cover, and the concentration of heavy industries like fertilizer, cement, steel, and thermal power plants (Narula et al. 2018). The region-specific climate affects the monsoonal rainfall, in turn, results with irregular rainfall, which induces variability ranging from small to large scale. The small-scale variability may be responsible for wet whereas a large scale is for both the situations (wet and drought). Similarly, for the brevity, the results of extreme droughts of scale 6- and -24 month are not presented. Similar observation is also noticed in three-time domains.

The results of extreme wet are presented in Fig. 5, in which the subplot of Fig. 5(a), (b), and (c) represent for a 3-month scale, whereas Fig. 5(d), (e), and (f) show the results of a 12-month scale. The results reveal that class 3 and 4 frequencies of extreme wet at a 3-month scale are found to be clustered in the Northeast, South-west coast region, and sparsely located in western parts of India over the FTD period. During this period, Southeast and some parts in central India experienced class 2 frequency of wet events. In STD, it is noticed that there exists a transition between low to high-class frequency of extreme wet events, in turn, most of the grids have experienced with class 3 and 4 frequencies. In TTD, it is found that the class 1 and 2 frequencies dominate over the Northeast-central and eastern part of India. Similarly, class 3 and 4 frequencies of extreme wet are found in West, Southwest coast and West-central part of India. From this, it is obtained that as the time window moves from FTD to TTD, the westward movement of wet events is seen at a 3-month scale. However, at the large time scale, class 3 and 4 frequencies of wet events are found in

439 the North and South region in FTD. In TTD, the most of events are found to be cluster over the
440 East-central and some parts in the South of India.

441 **3.1.4 Vulnerability index of rainfall extremes**

442 The proposed model explained in Section 2.2.3 is employed to quantify the vulnerability to rainfall
443 extremes over each of the grids. The classification of grids based on the calculated index for
444 extreme drought is presented in Fig. 6, in which subplot Fig. 6(a) and Fig. 6(b) represents for 3-
445 and 12-month scale. The results reveal that at 3- month scale, the high index (the upper quartile)
446 values are found to form a cluster in North-central, East, and East-central parts of India, whereas
447 low (lower quartile) index values are located in West, some grids in South of India. The
448 intermediate index values are located in some parts in the Peninsular, Northeast, and North regions.
449 On contrary, at a 12-month scale, the high index value for extreme droughts are found to form
450 clusters in West, West-coast, and Northcentral region of India, hence relatively high vulnerable
451 towards the extreme droughts. The region of Southeast coast, some parts in Northeast and North
452 receives low index values, hence relatively less vulnerable to extreme droughts. It is seen that
453 vulnerable regions concerning extreme droughts events depend on time scales. These vulnerable
454 regions are closely matched with the results mentioned in Shewale and Kumar (2005). It is reported
455 in Shewale and Kumar (2005) that these regions have been experiencing frequent droughts over
456 the last century. From the above analysis, it is concluded that at short scales such as 3-month, the
457 vulnerable regions concerning extreme droughts are found to be in Central and Northeast of India,
458 which is rich in agriculture activities, indicating potential threats in food security and socio-
459 economic factors (Mallya et al. 2016; Seitinthang 2014). Further, at a 12-month scale, the
460 vulnerable regions are found to be in Northcentral, West, and West-coast, indicating a threat to the
461 biodiversity and carbon sink at Western Ghats (Jena and Azad 2019; Murugan et al. 2009;

462 Manjunatha et al. 2015). Moreover, it was also found that the Western Ghat region has experienced
463 several temperatures mean change years and corresponding hotspot (Narula et al., 2018), which
464 was consistent with the present results at a 12-month scale.

465 Similarly, the vulnerability index for extreme wet are calculated at 3- and 12- month scales, and
466 the corresponding results are shown in Fig. 6, in which subplot Fig. 6(c) and Fig. 6(d) represents
467 for 3-month and 12-month, respectively. It is seen that the West, North, Southwest coast and
468 Northeast region experienced high index values at a 3-month scale, whereas Northeast-central and
469 some grids in West and Peninsular region regions receive intermediate index values. Similarly,
470 the region South, Southeast coast, Southwest coast, Central part, and Peninsular region of India
471 have experienced high index values at a 12-month scale. Further, the region Northeast, Northeast
472 Central, Northwest, West of India receive low index values at a 12-month scale.

473 **3.2 Results of CMIP5 Models**

474 **3.2.1 All-India projection of ensemble model:**

475 To preserve the stationarity in data, the long time series of rainfall data is split into three disjoint
476 parts in such a way that each part of data is sufficient for climate studies. The SPI is implemented
477 over each part of rainfall data at 3-, and 12-month. There will be a decadal gap in the occurrence
478 of 3-month droughts between 2060-2090 and 2030-2090 for 12-month droughts. A similar result
479 is reported in Preethi et al. (2019) mentioned that most of the droughts will occur in mid of the
480 future and its trend will decrease towards the end of the 21st century. However, their study has
481 included the moderate and severe drought, whereas the present study focuses on extreme droughts.
482 Similarly, the extreme wet events are extracted and the results reveal that the extreme wet events
483 at 3- and 12-month scales are like to occur frequently after 2060, which is inversely correlated

484 with the extreme drought events. Hence, it may be concluded that the drought events would
485 dominant over the early and mid of future, whereas wet events are like to dominant over the mid
486 and late 21st century at a 12-month scale. Similarly, at a 3-month scale, the drought events are like
487 to occur more frequently in 2020-2060, and thereafter, the wet events are likely to occur with high
488 frequency.

489 **3.2.3 Severity assessment of extreme drought and wet years in future**

490 Using the proposed model as mentioned in Fig. 1, the severity of extreme drought years is
491 calculated. The corresponding results are shown in Fig. 7, in which the upper panel shows for 3-
492 and 12-month of extreme droughts; and the lower panel represents the same for extreme wets. It
493 is seen that the extreme drought 2009 at 3- and 12-month scale has high severity index. Moreover,
494 it has been reported that the drought year 2009 was one of the most prominent over the past decades
495 (Preethi et al. 2019; Mallya et al. 2016), which supports one of our results. Based on the severity
496 index at a 3-month scale, the drought year 2036 and 2043 would be the most prominent extreme
497 drought years, which is likely to have an adverse impact in the future. Similarly, the highly
498 impacted extreme drought years at the 12-month scale will be 2026, 2037, and 2024, 2027, 2035,
499 respectively. It may be noted that most of the drought events would occur in the mid of the future
500 and their frequency will decrease at the end of the 21st century as shown in Fig. 7.

501 Similarly, the severity of extreme wet events is calculated and is presented in the lower panel of
502 Fig. 7. The results reveal that at a 3-month scale, the most prominent wet event years will be 2038,
503 2079, 2084, 2090, and 2099, in which 2079 and 2090 will have high impact followed by 2099.
504 Similarly, at 12- month scale the most impacted wet events will be 2085, 2092, 2094, 2100, and
505 2085, 2092, 2093, 2094, respectively, as evident from the high severity index shown in Fig. 7.
506 From this analysis, it is obtained that India is likely to experience most impacted wet events after

507 2070, whereas it will have fewer impacted wet events in the early part of the 21st century. On
508 contrary to this, the entire India would experience high impacted extreme drought events in the
509 early part of the 21st century and its frequency will decrease towards the end of the 21st century.

510 **3.2.4 Gridded scale**

511 The Spatio-temporal shift of extreme events is analyzed over three disjoint periods such as 2006-
512 2035 (future first-time domain, (FFTD)), 2036-2070 (future second-time domain, (FSTD)) and
513 2071-2100 (future third-time domain, (FTTD)). The analyses over FFTD facilitate the early
514 occurrence of the extreme events, FSTD is for mid-future, and FTTD is for the end of the 21st
515 century. The results at a 3- and 12- month scale are presented in Fig. 8 and it reveals that in FFTD
516 some grids in West, Northeast, and Central regions of India are likely to experience class 4
517 frequency of extreme droughts at 3-month scale. Further, the class 3 and 4 frequencies of extreme
518 droughts cover the entire region of India during FSTD and finally, class 4 frequency of extreme
519 droughts would form a dense cluster over the West Coast, West and West central region in FTTD.
520 Similarly, the results of the 12-month scale reveal that the regions of Peninsular, Southeast coast,
521 and central region will like to experience class 4 frequency of extreme droughts during FFTD.
522 Further, the class 4 frequency is likely to shift towards the North and Northcentral region during
523 FSTD. It is noticed that there will no more class 4 frequency of extreme droughts, however, the
524 class 3 frequency will dominate in the region of West and West central region during FTTD. It is
525 obtained that in FSTD, the whole region will experience droughts with high frequency at a 3-
526 month scale, whereas North and Northcentral will only experience 12-month droughts. Also, it is
527 noticed that the frequency of either drought decreases towards the end of the 21st century. Most of
528 the impacted drought years are found to cluster in FFTD and there will be few impacted drought
529 years in FTTD. Further, it supports the results reported in Preethi et al. (2019) that India will

experience increased frequency of drought in early and mid-future (up to 2069). Moreover, the identified regions, which are likely to receive a high class of drought frequency also matches with earlier reports in Preethi et al. (2019) and Ojha et al. (2013) that the West Central, Peninsular, and Central Northeast regions of India, whereas the northern part of India and coastal regions, would receive a high class of extreme wet events frequency.

Similarly, the frequency of classes of wet events is shown in Fig. 9 at 3- and 12-month scales. It is obtained that the West-central part and Northcentral of India are like to experience a high frequency of extreme wet in FFTD at a 3-month scale. Similarly, in the FSTD central part, the northeast region and some grids in the western region are like to experience low frequency of extreme wet events. During FTTD, the South, East, Central, and Peninsular region of India would like to experience a relatively high frequency in comparison to other parts of India. It is also obtained that the North and Northcentral parts of India are likely to experience a low frequency of extreme wet events. Similarly, at a 12-month scale, the West Coast, South, Peninsular, and East-central parts of India would have a high frequency of extreme wet, whereas the North and Northcentral region would experience low frequency of extreme wet events.

3.3.4 Vulnerability index of rainfall extremes

The proposed model defined in Fig. 2 is employed to calculate the vulnerability index at each grid. The classification of grids based on index values of extreme droughts is shown in Fig. 10 (upper panel) at 3- and 12-month scales. It reveals that at a 3-month scale the region Northeast, Northeast Central, East Coast, and some grids in South part of India are likely to have high index values, hence would experience high frequency, prolonged droughts with high intensity. Consequently, it would adversely impact agriculture over these regions, threatening the food security over the region as well as in the entire country. Also, at a 12-month scale, the high index values are likely

553 to form clusters over West, Northwest, Northcentral, and some parts in the Northeast region. These
554 regions have witnessed several agricultural activities such as rice, sugarcane, etc. which depend
555 on a significant amount of rainfall. Also, there are many small water reservoirs over these regions,
556 which are more likely to be affected. The deficit of accumulated rainfall at 3-month scale directly
557 impact agricultural activities, especially rice and small water reservoir. The deficit of accumulated
558 rainfall at 12-month would impact the water reservoir and groundwater level, consequently, it
559 would affect the hydroelectric generation and hence the urban lives are likely to experience an
560 adverse situation in the future. From this, it is observed that the region Northeast, East Coast,
561 Northwest central, and North of India would be vulnerable to extreme drought conditions at small
562 scales, whereas, it is found that at large scale the West coast and West-central will be the vulnerable
563 regions.

564 Vulnerable index for extreme wet events is calculated at 3- and 12- month scales and the
565 corresponding results are depicted in Fig. 10 (lower panel). It is seen some grids in the Northeast,
566 West, West Coast and some grids in the Peninsular region will have high index values at a 3-month
567 scale. Moreover, it is seen that these regions are likely to receive low drought index value which
568 supports the inverse relation of occurrence of drought and wet events. Similarly, at 12- month scale
569 West, Peninsular, East Coast and South part of India will have high index values, hence are likely
570 to be the most vulnerable regions.

571 **4. Discussions and conclusions**

572 The Indian monsoon rainfall has been experiencing frequent occurrences of extreme events during
573 recent decades, especially from 1960 onwards. Notably, the year 2002, 2004, and 2009, were the
574 most extended droughts that occurred over India in the decade of 2000-2010 (Preethi et al. 2019,
575 Mallya et al. 2014). To identify the highly impacted extreme events, a conceptual model is

576 proposed, as mentioned in Fig. 1 and employed over each part of the time. The calculated values
577 show the severity of the extreme events and based on the high index values; it is obtained that
578 1905, 1907, 1918, 1959, 1964-65, 1971-72, 2000-02, and 2008 were the most impacted extreme
579 drought years over last 20th century. A decadal gap of occurrence of severely impacted droughts
580 at short/large time scales is found in the period 1921-1959. There are many factors involved in the
581 mechanism of large-scale droughts such as global changes, thermodynamic feedback due to
582 heating rates (Roxy et al. 2015). The changes in Indian and global temperatures could likely affect
583 thermodynamic heating/cooling rates, consequently, affecting the monsoon active and dry spell.
584 Further, the dry spells (there is no rain for five or more consecutive days) has been increased; light
585 precipitation days have significantly decreased; consequently, the drought indices have been
586 changing after the post-global warming (Mishra and Liu 2014). These changes could have also
587 been influenced by natural forcing like Indian Ocean Dipole (IOD), El Niño–Southern Oscillation
588 (ENSO), and internal variability of monsoon (Mishra and Liu 2014). However, rainfall events are
589 time and space localized, and the mechanism of forming such events is still in conjecture. During
590 1950-2005, the global mean temperatures and Indian mean temperatures have changed three to
591 four times (Narula et al. 2018). It has been noticed that the most impacted droughts have occurred
592 after the global warming era. Further, the based on the high severity index values the years 1906,
593 1914, 1916-17, 1932, 1946 1955, 1970, 1977, 1989, 1997, 2005, 2009 and 2012 are most impacted
594 wet years. These results closely match Preethi et al. (2019), Parthasarathy et al. (1994), Bhalme &
595 Mooley (1980), and Dhar & Nandargi (2003).
596 Climate models are considered as the primary tool for estimating future projections and provide
597 data up to the 21st century. The present study has examined 12 selected climate model data that
598 have captured observed climatology of Indian monsoon rainfall (Jena et al. 2015, 2016; Jena and

599 Azad 2019). Further, these climate models are used to generate an ensemble model and is used for
600 future analysis. The proposed model (Fig. 1) is implemented to quantify the most impacted
601 extreme events that are likely to occur in the future. Based on the high severity index values, the
602 years 2036 and 2043 at 3-; 2026 and 2037 at a 12-month scale will be impacted extreme drought
603 in the future. Similarly, the most prominent wet years will in 2038, 2067, 2075-76, 2079-80, 2084-
604 85, 2090-92, and 2099 over all time scales.
605 Furthermore, given the need for classification of grids concerning extreme droughts and wet, a
606 new vulnerable index has been proposed (Fig. 2), which consolidates the outcomes of SPI such as
607 frequency, prolonged duration, and magnitude. In addition to this, the proposed model assigns
608 various weights to grids to incorporate the global warming effect, which is an important indicator
609 to identify the vulnerable region. Based on the high index values, it is found that Peninsular,
610 Northeast, North regions, West, West-coast, and Northcentral part of India are vulnerable to
611 extreme drought events. These results are in agreement with the findings of Shewale and Kumar
612 (2005) that these regions are prone to frequent drought. Further, these regions are rich in
613 agriculture activities, indicating potential threats in food security, socio-economic factors (Mallya
614 et al. 2016; Seitinthang 2014), bio-diversity and carbon sink (Jena and Azad 2019; Murugan et al.
615 2009; Manjunatha et al. 2015). Based on the projection simulation of climate models, the
616 vulnerable region concerning extreme drought are summarized as follows:

617 • Northeast, Northeast Central, East Coast, and some grids in South part of India are likely
618 to have high index value, hence they are likely to experience high frequency, prolonged
619 droughts with high intensity.
620 • At a 12-month scale, the high index is likely to form clusters over West, Northwest,
621 Northcentral, and some parts in the Northeast region.

Further findings of vulnerable regions respect to extreme wet events are as follows:

- Northeast, West, West Coast, and some grids in the Peninsular region will have high index values at a 3-month scale.
- Similarly, at 12- month scale West, Peninsular, East Coast and South part of India will have high index values, hence it will be the most vulnerable region.

The identified vulnerable regions may be useful for policymakers, agriculture planning, and water resource management.

Appendix

1. Selection of probability distribution function for the fitting of data

As it is mentioned in Thom (1958) and Wilks (1995) that the gamma distribution is a good choice for describing precipitation values at different time scales for a variety of reasons. The advantage of the gamma distribution includes firstly, it is bounded on the left at zero and the gamma distribution is positively skewed, meaning that it has an extended tail to the right of the distribution. Many studies have employed the gamma distribution in the analysis of rainfall. It is reported that the maximum likelihood estimators (MLEs) optimally calculate the shape and scale parameters for the gamma distribution. An alternative to the MLE parameters is the method of moment estimation (MME). It has been shown, however, that the method of moments is a poor estimator, owing to inefficiency, for small shape values (Wilks 1995; Thom 1958). Further, the present study has applied various distributions to fit the rainfall data at different time scales. To verify the efficiency of the distribution, Akkai information criteria (AIC) is calculated for all different data sets and the result is mentioned in Table A1 and Table A2. It reveals that the gamma distribution performs uniformly over all kinds of datasets. A rank is assigned to each of distribution based on the

performance (best fitting) and mentioned in Table A2, it reveals that the gamma distribution score lowest rank, represents best fit for the rainfall data.

Table A1: Calculated AIC values for various distribution fitted at different time scales of data

Distribution	Monthly	3-month	24-month
Weibull	14876.53	17857.30	16061.77
Gamma	14882.46	17831.50	15961.00
Logistics	16138.86	18752.29	16002.00
Normal	16102.46	18657.63	15956.51
Lognormal	14833.49	17853.40	15968.72

Table A2: Rank of the distribution's performance in fitting data at different time scales

Distribution	Monthly	3-month	12-month	Final
Weibull	2	3	4	9
Gamma	3	1	1	6
Logistics	5	5	5	15
Normal	4	4	2	10
Lognormal	1	2	3	5

References:

Azad S, Rajeevan, M (2016) Possible shift in the ENSO-Indian monsoon rainfall relationship under future global warming. Scientific Rep 6, 20145.

Becker A, Finger P, Meyer-Christoffer A, Rudolf B, Schamm K, Schneider U, & Ziese M (2013) A description of the global land-surface precipitation data products of the Global Precipitation Climatology Centre with sample applications including centennial (trend) analysis from 1901-present. Earth Syst Sci data 5(1):71.

Bhalme HN, Mooley DA, Jadhav SK, 1983. Fluctuations in the drought/wet area over India and relationships with Southern Oscillation. Mon Weather Rev 111 (1):86–94.

Bhalme HN, & Mooley DA (1980) Large-scale droughts/wets and monsoon circulation. Mon Weather Rev 108(8):1197-1211.

Bonaccorso B, Bordi I, Cancelliere A, Rossi G, Sutera A (2003) Spatial variability of drought: and analysis of the SPI in Sicily. Water Resour Manag 17:273–296.

Brooks N, Adger W, and Kelly P (2005) "The determinants of vulnerability and adaptive capacity at the national level and the implications for adaptation." Global Environ Change 15(2):151–163.

Cook BI, Ault TR, Smerdon JE (2015) Unprecedented 21st century drought risk in the American Southwest and Central Plains. Sci Adv 1(1): e1400082.

Dabanli I (2018) Drought hazard, vulnerability, and risk assessment in Turkey. Arab J Geosciences 11 (18): 538.

Dickey DA, and Fuller WA (1981) Fuller Likelihood ratio statistics for autoregressive time series with a unit root Econometrica. 49:1057-1072.

Diffenbaugh NS, & Giorgi F (2012) Climate change hotspots in the CMIP5 global climate model ensemble. Clim change 114(3-4):813-822.

673 Dhar ON, & Nandargi S (2003) Hydrometeorological aspects of wets in India. Nat Hazards
674 28(1):1-33.

675 Eakin H, and Conley J (2002) "Climate variability and the vulnerability of ranching in southeastern
676 Arizona: A pilot study." Clim Res 21(3):271–282.

677 Edwards DC, McKee TB (1997) Characteristics of 20th century drought in the United States at
678 multiple time scales. Climatology Rep 97-2. Colorado State University Department of
679 Atmospheric Science Fort Collins Colorado, p 155.

680 Fowler AM, Hennessy KJ (1995) Potential impacts of global warming on the frequency and
681 magnitude of heavy precipitation. Nat Hazards 11 (3):283-303.

682 Geil KL, Serra YL, & Zeng X (2013) Assessment of CMIP5 model simulations of the North
683 American monsoon system. J Clim 26(22):8787-8801.

684 Harris I, Jones PD, Osborn TJ, Lister DH (2014) Updated high-resolution grids of monthly climatic
685 observations–the CRU TS3 10 dataset. Int J Climatol 34 (3):623–642.

686 Hayes MJ, Svoboda MD, Wilhite DA, Vanyarkho OV (1999) Monitoring the 1996 drought using
687 the standardized precipitation index. Bull Am Meteor Soc 80:429–438.

688 IPCC 1996: Climate Change 1995. The science of climate change, Contribution of Working Group
689 One to the Second Assessment Report of the Intergovernmental Panel on Climate Change,
690 Cambridge University Press, Cambridge, 531 pp.

691 IPCC 2001: Climate Change 2001. The scientific basis, In: J. T. Houghton, Y. Ding, D. J. Griggs,
692 M. Noguer, P. J. van der Linden, X. Dai, K. Maskell and C. A. Johnson (eds), Contributions of
693 working Group I to the Third Assessment Report of the Intergovernmental Panel on Climate

694 Change, Cambridge University Press, Cambridge, United Kingdom and New York, NY, USA, 881
695 pp.

696 Jena P, Azad S, Rajeevan MN (2015) Statistical selection of the optimum models in the CMIP5
697 dataset for climate change projections of Indian monsoon rainfall. Climate 3 (4):858–875.

698 Jena P, Azad S, Rajeevan MN (2016) CMIP5 projected changes in the annual cycle of Indian
699 monsoon rainfall. Climate 4:1-14.

700 Jena P, Azad S (2019) Weakening of triennial oscillation of the Indian summer monsoon rainfall
701 (at $1^o \times 1^o$ gridded scale) under future global warming. Earth and Space Sci 6 (7):1262-1272.

702 Jena P, Kasiviswanathan KS, & Azad, S (2020) Spatiotemporal characteristics of extreme droughts
703 and their association with sea surface temperature over the Cauvery River basin, India. Nat
704 Hazards 1-21.

705 Jones PD et al. (2012) Hemispheric and large-scale land-surface air temperature variations: an
706 extensive revision and an update to 2010. J Geophys Res 117: D05127.

707 Kar SK, Thomas T, Singh RM, Patel L (2018) Integrated assessment of drought vulnerability using
708 indicators for Dhasan basin in Bundelkhand region, Madhya Pradesh, India. Curr Sc 115 (2): 338-
709 346.

710 Kim H, Park J, Yoo J, Kim TW (2015). Assessment of drought hazard, vulnerability, and risk: A
711 case study for administrative districts in South Korea. J Hydro-Environ Res 9(1): 28-35.

712 Koirala S, Hirabayashi Y, Mahendran R, & Kanae S (2014) Global assessment of agreement
713 among streamflow projections using CMIP5 model outputs. Environ Res Lett 9(6): 064017.

714 Lavell A, Oppenheimer M, Diop C, Hess J, Lempert R, Li J, Muir-Wood R, Myeong S, Moser S,
715 Takeuchi K, Cardona OD, Hallegatte S, Lemos Maria, Little C, Lotsch A, Weber E (2012) Climate
716 change: new dimensions in disaster risk, exposure, vulnerability, and resilience. In: Field CB,
717 Barros V, Stocker TF, Dahe Q (Eds.), Managing the Risks of Extreme Events and Disasters to
718 Advance Climate Change Adaptation: Special Report of the Intergovernmental Panel on Climate
719 Change. Cambridge University Press, pp. 25–64.

720 Mallya G, Mishra V, Niyogi D, Tripathi S, Govindaraju RS (2016) Trends and variability of
721 droughts over the Indian monsoon region. Weather and Clim Extr 12: 43-68.

722 Manikandan M, Tamilmani D (2013) Development of drought vulnerability maps in the
723 Parambikulam-Aliyar Basin, Tamil Nadu, India. Scientific Res Essays 8 (20): 778-790.

724 Manjunatha BR, Balakrishna K, Krishnakumar KN, Manjunatha HV, Avinash K, Mulemane AC,
725 Krishna KM (2015) Increasing trend of rainfall over Agumbe, Western Ghats, India in the scenario
726 of global warming. Open Oceanography J 8(1):39-44.

727 McKee TB, Doesken NJ, Kleist J (1993) The relationship of drought frequency and duration to
728 time scales. In Proceedings of the 8th Conference on Applied Climatology. AMS: Boston, MA;
729 179–184.

730 Meehl GA, Arblaster JM, Tebaldi C (2005) Understanding future patterns of precipitation intensity
731 in climate model simulations. Geophys Res Lett 32: L18719.

732 Metzger MJ, Leemans R, Schro¨ter D (2005) A multidisciplinary multiscale framework for
733 assessing vulnerabilities to global change. Int J Appl Earth Obs 7:253e267.

734 Mishra A, Singh V (2010) A review of drought concepts. J Hydrol 391:202–216.

735 Mishra A, & Liu SC (2014). Changes in precipitation pattern and risk of drought over India in the
736 context of global warming. J Geophys Res-Atmos 119(13):7833-7841.

737 Mooley DA (1973) Gamma distribution probability model for Asian summer monsoon monthly
738 rainfall. Mon Weather Rev 101: 160–176.

739 Murugan M, Shetty PK, Anandhi A, Ravi R, Alappan S, Vasudevan M, Gopalan S (2009) Rainfall
740 changes over tropical montane cloud forests of southern Western Ghats, India. Curr Sci 1755–
741 1760.

742 Murthy CS, Laxman B, Sai MS (2015) Geospatial analysis of agricultural drought vulnerability
743 using a composite index based on exposure, sensitivity and adaptive capacity. International Journal
744 of Disaster Risk Reduction, 12, 163-171.

745 Nagarajan R (2003) Drought Assessment, Monitoring, Management & Resources Conservation,
746 Capital Publishing Co., Bangalore, India, 1–32.

747 Narasimhan B, Srinivasan R (2005) Development and evaluation of Soil Moisture Deficit Index
748 (SMDI) and Evapotranspiration Deficit Index (ETDI) for agricultural drought monitoring. Agric
749 For Meteor 133:69–88.

750 Narula P, Sarkar K, Azad S (2018) A functional evaluation of the spatiotemporal patterns of
751 temperature change in India. Int J Climatol 38(1): 264–271.

752 Oikonomou PD, Tsesmelis DE, Waskom RM, Grigg NS, Karavitis CA (2019) Enhancing the
753 standardized drought vulnerability index by integrating spatiotemporal information from satellite
754 and in situ data. J Hydro 569:265-277.

Ojha R, Nagesh Kumar D, Sharma A, Mehrotra R (2013) Assessing severe drought and wetevents over India in a future climate using a nested bias-correction approach. J Hydrol Eng 18 (7):760-772.

Orlowsky B, Seneviratne SI (2013) Elusive drought: Uncertainty in observed trends and short-and long-term CMIP5 projections. Hydrol Earth Syst Sci 17:1765–1781.

Parthasarathy B, Sontakke NA, Munot AA, KoPaithawale DR (1987) Droughts/wets in summer monsoons season over different meteorological sub-divisions of India for the period 1871–1980. J Climatol 7:57–70.

Parthasarathy B, Munot AA, Kothawale DR (1994) All India monthly and seasonal rainfall series 1871–1993. Theor Appl Climatol 49:217–224.

Peters E, Van Lanen HAJ, Torfs PJJF, Bier G (2005) Drought in groundwater—drought distribution and performance indicators. J Hydrol 306 (1-4): 302-317.

Preethi B, Ramya R, Patwardhan SK, Mujumdar M, Kripalani, RH (2019) Variability of Indian summer monsoon droughts in CMIP5 climate models. Clim Dyn 53(3-4):1937-1962.

Rajeevan M, Bhate J, Kale JD, Behera BLS, Krishnan R, Yamagata T (2006) High resolution daily gridded rainfall data for the Indian region: analysis of break and active monsoon spells. Curr Sci 91:296–306.

Rajeevan M, Bhate J, Jaswal AK (2008) Analysis of variability and trends of extreme rainfall events over India using 104 years of gridded daily rainfall data. Geophy Res Lett 35 (18).

774 Rao BB, Chowdary PS, Sandeep VM, Rao VUM, & Venkateswarlu B (2014) Rising minimum
775 temperature trends over India in recent decades: Implications for agricultural production. Glob
776 Planet Change 117: 1-8.

777 Robertson AW, M Bell R, Cousin et al. (2013) Online tools for assessing the climatology and
778 predictability of rainfall and temperature in the IndoGangetic Plains based on observed datasets
779 and seasonal forecast models. Working paper no. 27. CGIAR research program on Climate
780 Change, Agriculture and Food Security (CCAFS), Cali, Colombia.

781 Reeves Eyre JEJ, & Zeng X (2017) Evaluation of Greenland near surface air temperature datasets.
782 The Cryosphere 11:1591-1605.

783 Roxy MK, Ritika K, Terray P, Murtugudde R, Ashok K, Goswami BN (2015) Drying of Indian
784 subcontinent by rapid Indian Ocean warming and a weakening land-sea thermal gradient. Nat
785 Commun 6: 7423.

786 Samra JS (2004). Review and analysis of drought monitoring, declaration and management in
787 India (Vol. 84). IWMI.

788 Seitinthang L (2014) Cropping pattern of Northeast India: An appraisal. American Research
789 Thoughts 1 (1).

790 Shannon CE (1948) A mathematical theory of communication. Bell Syst. Tech J 27: 379–423.

791 Shi H, Li T, Wei J (2017) Evaluation of the gridded CRU TS precipitation dataset with the point
792 rain gauge records over the Three-River Headwaters Region. J Hyd 548: 322–332.

793 Shewale MP, Kumar S (2005). Climatological features of drought incidences in India.
794 Meteorological Monograph (Climatology 21/2005). National Climate Centre, Indian
795 Meteorological Department.

796 Sheffield J, Wood EF (2008) Projected changes in drought occurrence under future global
797 warming from multi-model, multi-scenario, IPCC AR4 simulations. Clim. Dyn. 31, 79–105.

798 Smit B, Burton I, Klein RJ, Street R (1999) The science of adaptation: a framework for assessment.
799 Mitig Adapt Strat Glob Chang 4:199–213.

800 Svoboda M, Fuchs B (2016) Handbook of drought indicators and indices. Integrated Drought
801 Management Programme (IDMP), Integrated Drought Management Tools and Guidelines Series
802 2. Geneva. World Meteorological Organization WMO-No. 1173

803 Swann ALS, Hoffman FM, Koven CD, Randerson JT (2016) Plant responses to increasing CO2
804 reduce estimates of climate impacts on drought severity. Proc Natl Acad Sci 113: 10019–10024.

805 Taylor K, Stouffer R, Meehl GA (2011) A Summary of the CMIP5 experiment design. 33.

806 Taylor KE, Stouffer RJ, Meehl GA (2012) An overview of CMIP5 and the experiment design.
807 Bull Am Meteor Soc 93:485–498.

808 Taylor IH, Burke E, McColl L, Falloon PD, Harris GR, McNeall D (2013) The impact of climate
809 mitigation on projections of future drought. Hydrol Earth Syst Sci 17: 2339–2358.

810 Thom, H.C., 1958. A note on the gamma distribution. Mon. Weather Rev. 86 (4), 117-122.

811 Thorne PW et al. (2016) Reassessing changes in diurnal temperature range: intercomparison and
812 evaluation of existing global data set estimates. J Geophys Res Atmos 121: 5138–5158.

813 Tsakiris G, & Vangelis H (2004) Towards a drought watch system based on spatial SPI. Water
814 resources management 18(1):1-12.

815 Tyalagadi, M. S., Gadgil, A., & Krishnakumar, G., 2015. Monsoonal droughts in India–a recent
816 assessment. Papers on Global Change, 22.

817 United Nation Development Program (2004) Reducing Disaster Risk: a Challenge for
818 Development. John S. Swift Co, New York.

819 Vasiliades L, Loukas A, Liberis N (2011) A water balance derived drought index for Pinios River
820 Basin, Greece. Water Resour Manag 25 (4):1087-1101.

821 Veijalainen N, Vehvilainen B (2008) The effect of climate change on design wets of high hazard
822 dams in Finland. Hydrol Res 39:465-477.

823 Wilks DS (1995) Statistical Methods in the Atmospheric Sciences: an Introduction. Academic
824 Press: San Diego, CA.

825 Willmott CJ, & Matsuura K (2001) Terrestrial air temperature and precipitation: monthly and
826 annual time series (1950–1999). Center for Climatic Research, Department of Geography,
827 University of Delaware.

828 Xie SP, Deser C, Vecchi GA, Ma J, Teng H, Wittenberg AT (2010) Global warming pattern
829 formation: Sea surface temperature and rainfall. J Clim 23 (4):966-986.

830 Yang JS, Park JH, Kim NK (2012) Development of drought vulnerability index using trend
831 analysis. Journal of The Korean Society of Civil Engineers 32(3B):185-192.

832 Zhang Q, Xu CY, Gemmer M, Chen YD, Liu CL (2008) Changing properties of precipitation
833 concentration in the Pearl River basin, China. Stoch Environ Res Risk Assess 23 (3):377-385.

834 Zhao T, Dai A (2015) The magnitude and causes of global drought changes in the twenty-first
835 century under a low moderate emissions scenario. J. Climate 28:4490–4512.

836

Figures

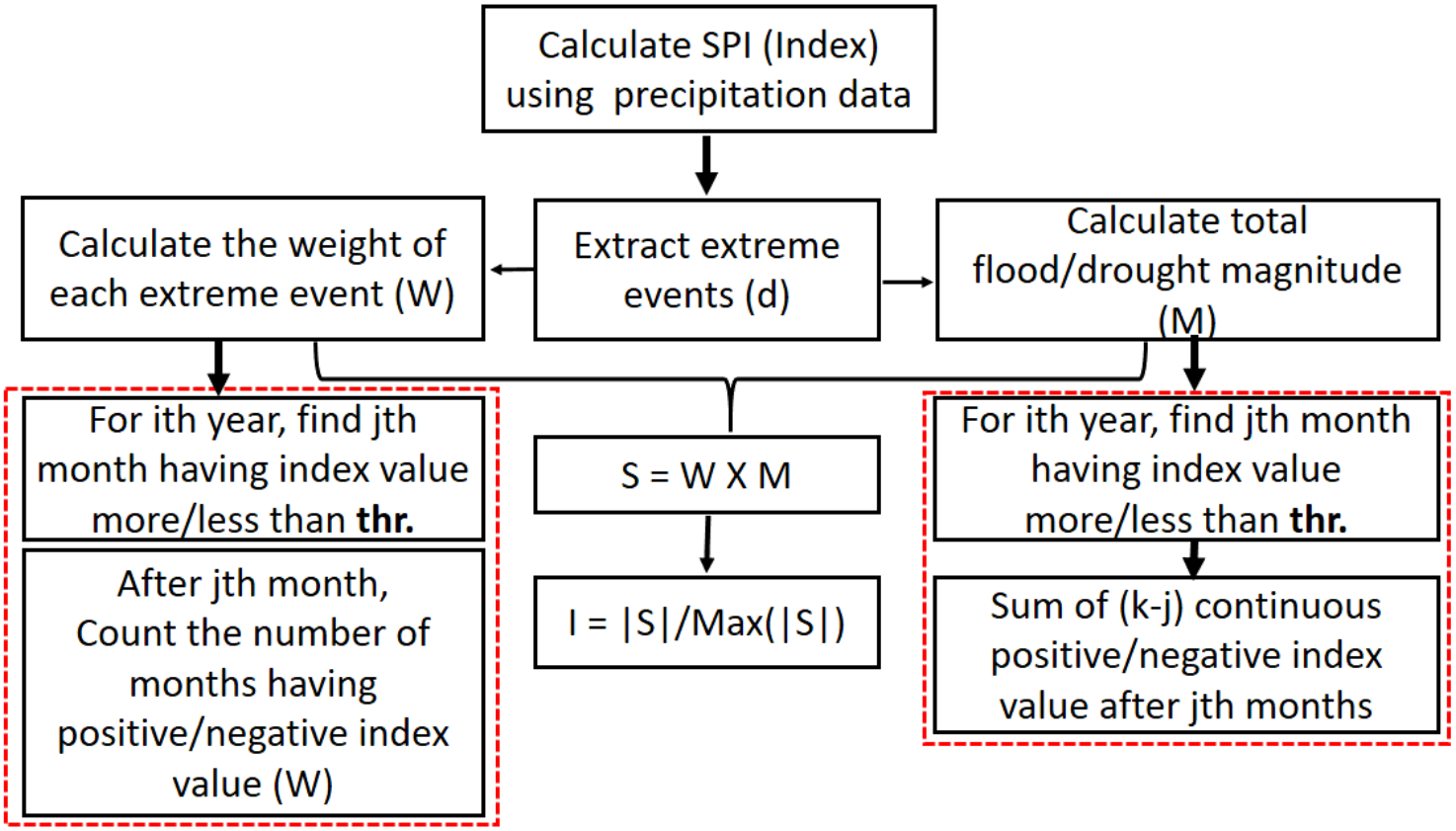

Figure 1

Procedure for calculating the severity of extreme drought and flood events over the study period (1901-2014 and 2006-2100).

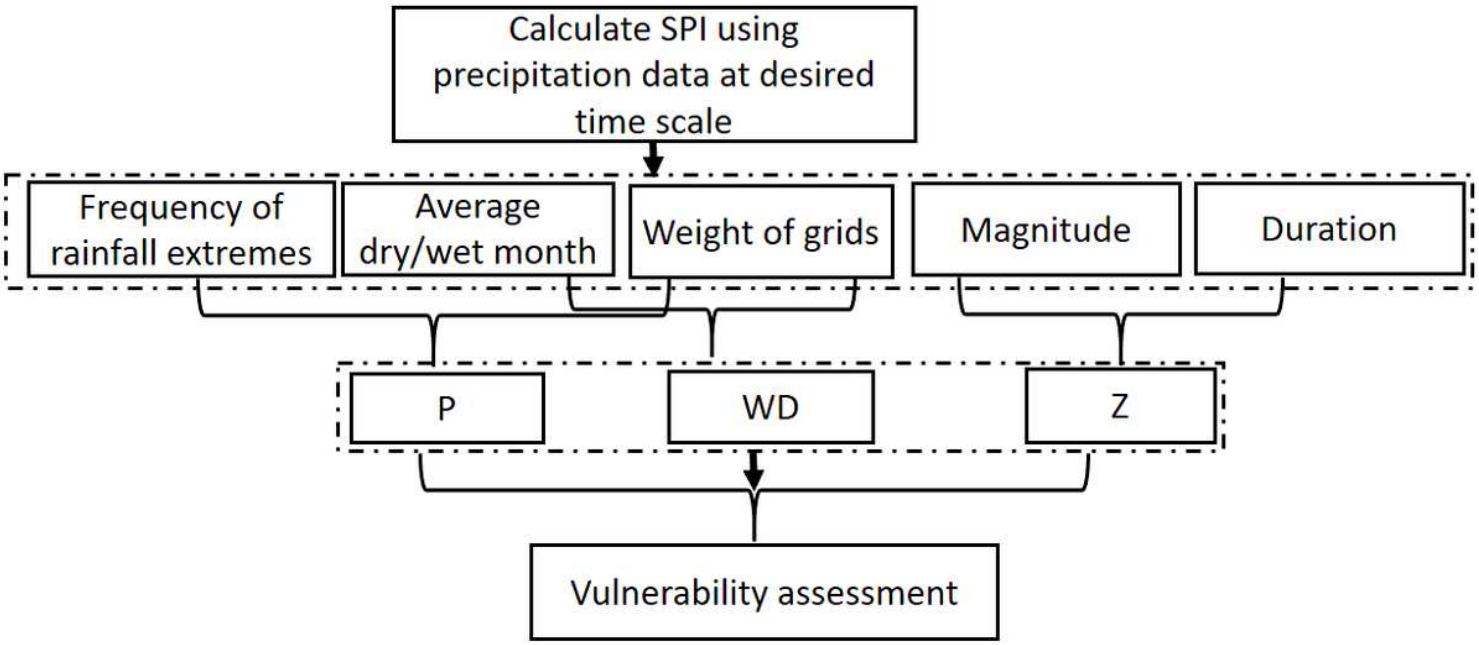

Figure 2

Procedure for calculating the vulnerability of the region concerning extreme drought and flood events over the study period (1901-2014 and 2006-2100).

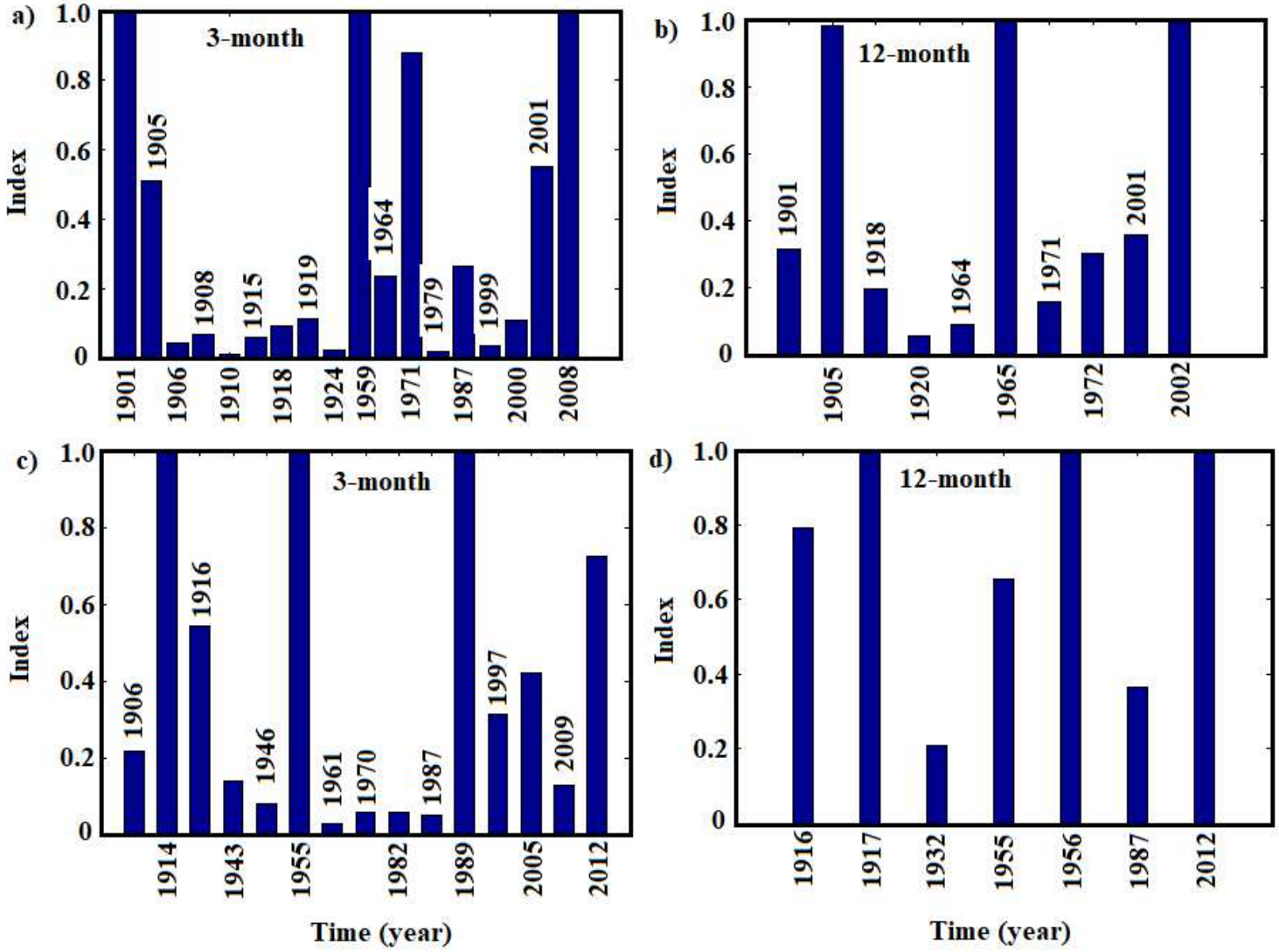

Figure 3

Assessment of severity of extreme drought years a) for at 3- month, b) for 12- month scales and extreme flood years c) for 3-month, d) for 12-month scales for 1901-2014.

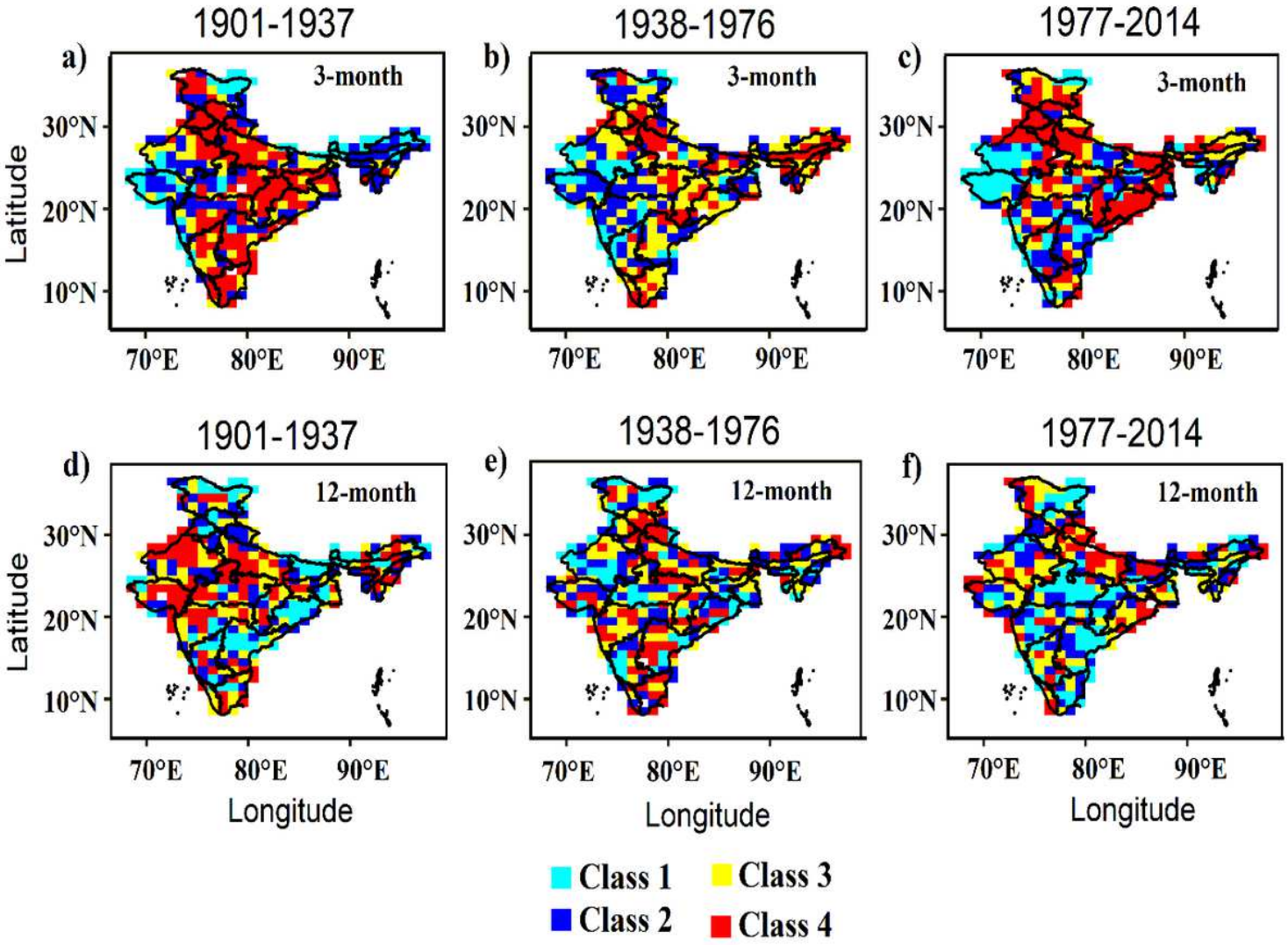

Figure 4

Spatial distribution of frequency of extreme drought years at 3- month scale for the time period: (a) 1901-1937; (b) 1938-1976; (c) 1977-2014. At 12-month scale: (d) 1901-1937; (e) 1938-1976; (f) 1977-2014.

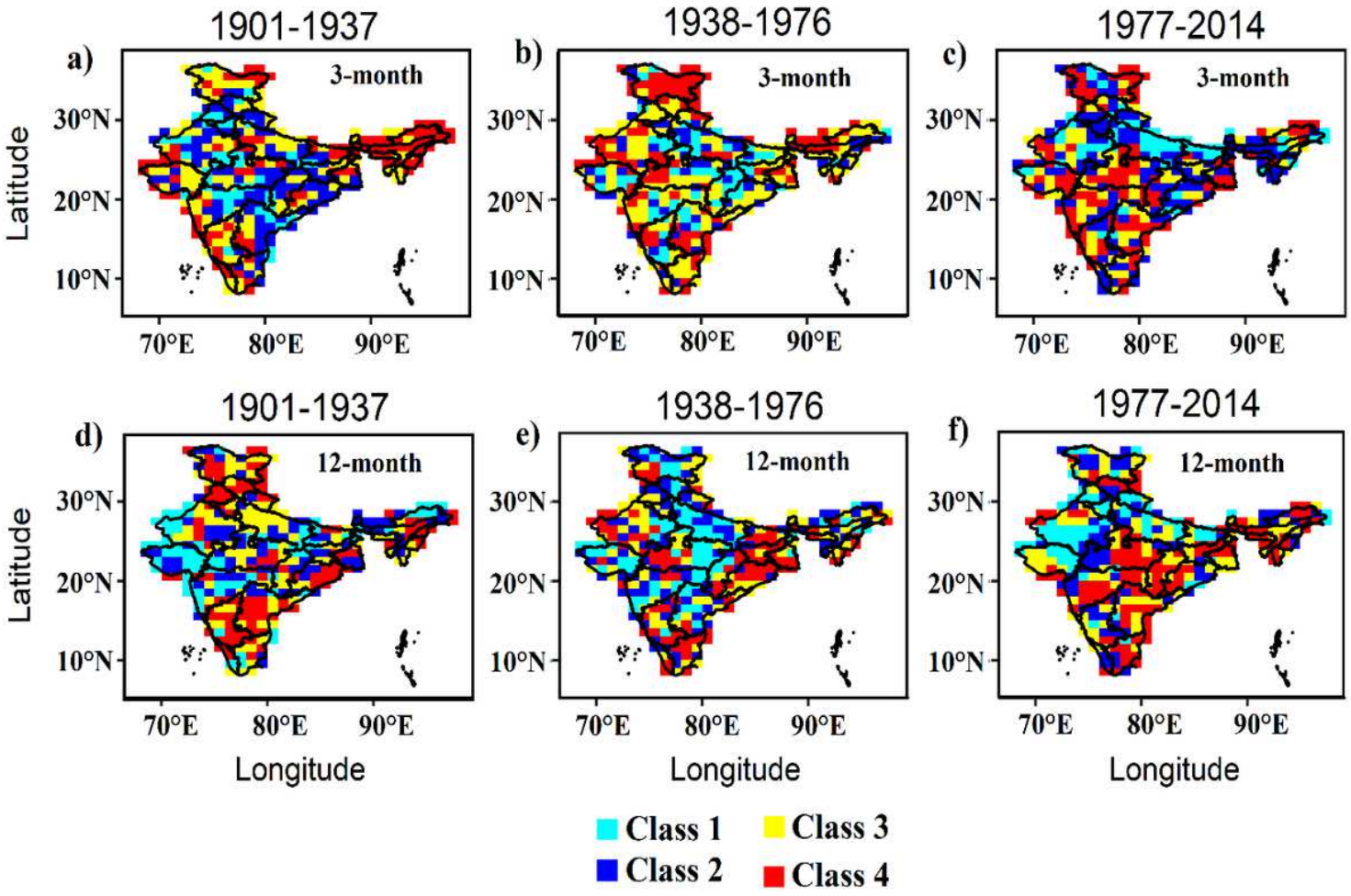

Figure 5

Spatial distribution of frequency of extreme flood years at 3- month scale for the time period: (a) 1901-1937; (b) 1938-1976; (c) 1977-2014. At 12-month scale: (d) 1901-1937; (e) 1938-1976; (f) 1977-2014.

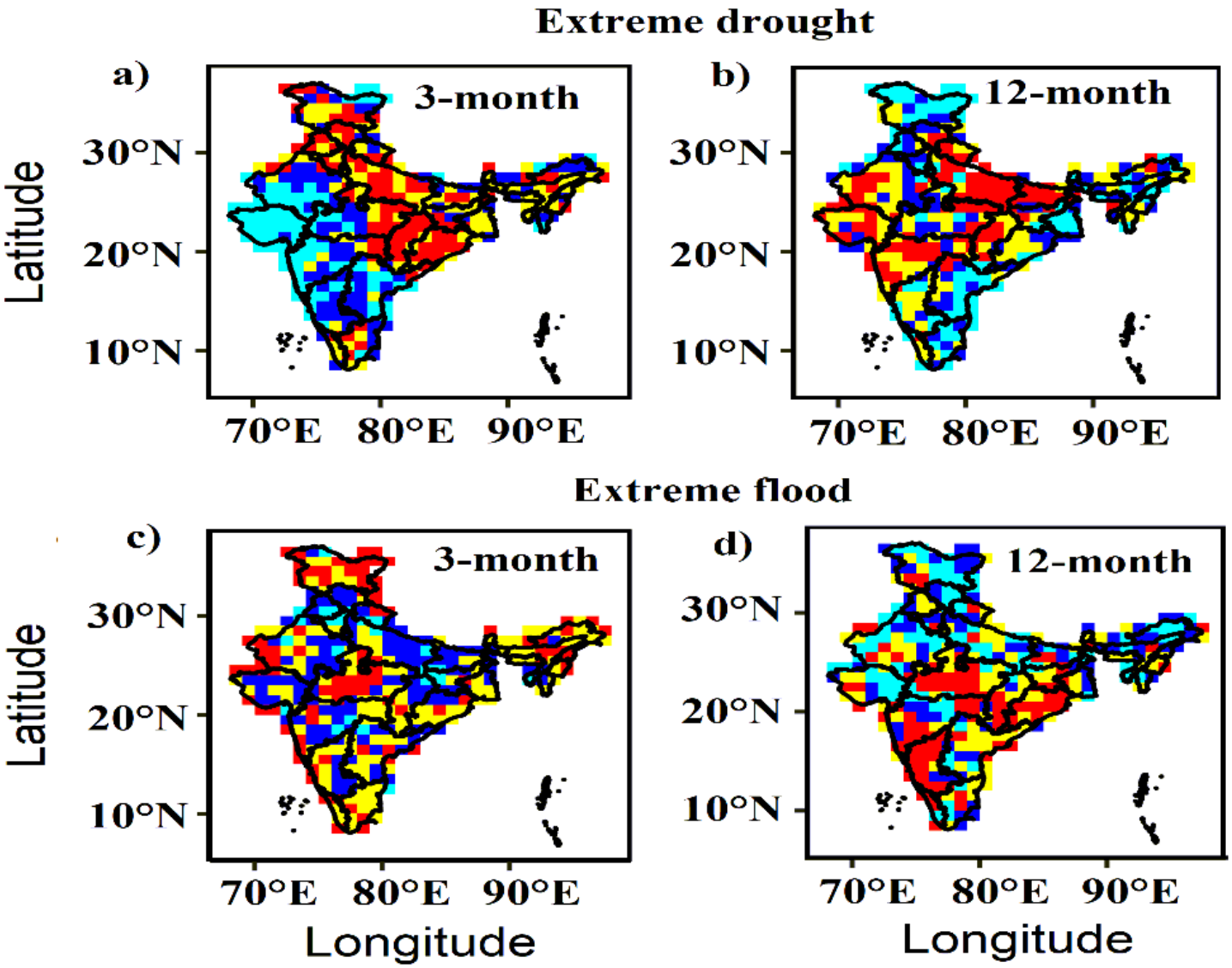

Figure 6

Classification of grids based on vulnerability index (I) of extreme drought (a) at 3- month; (b) at 12-month; and of extreme floods (c) at 3-month; (d) at 12-month scale for 1901-2014.

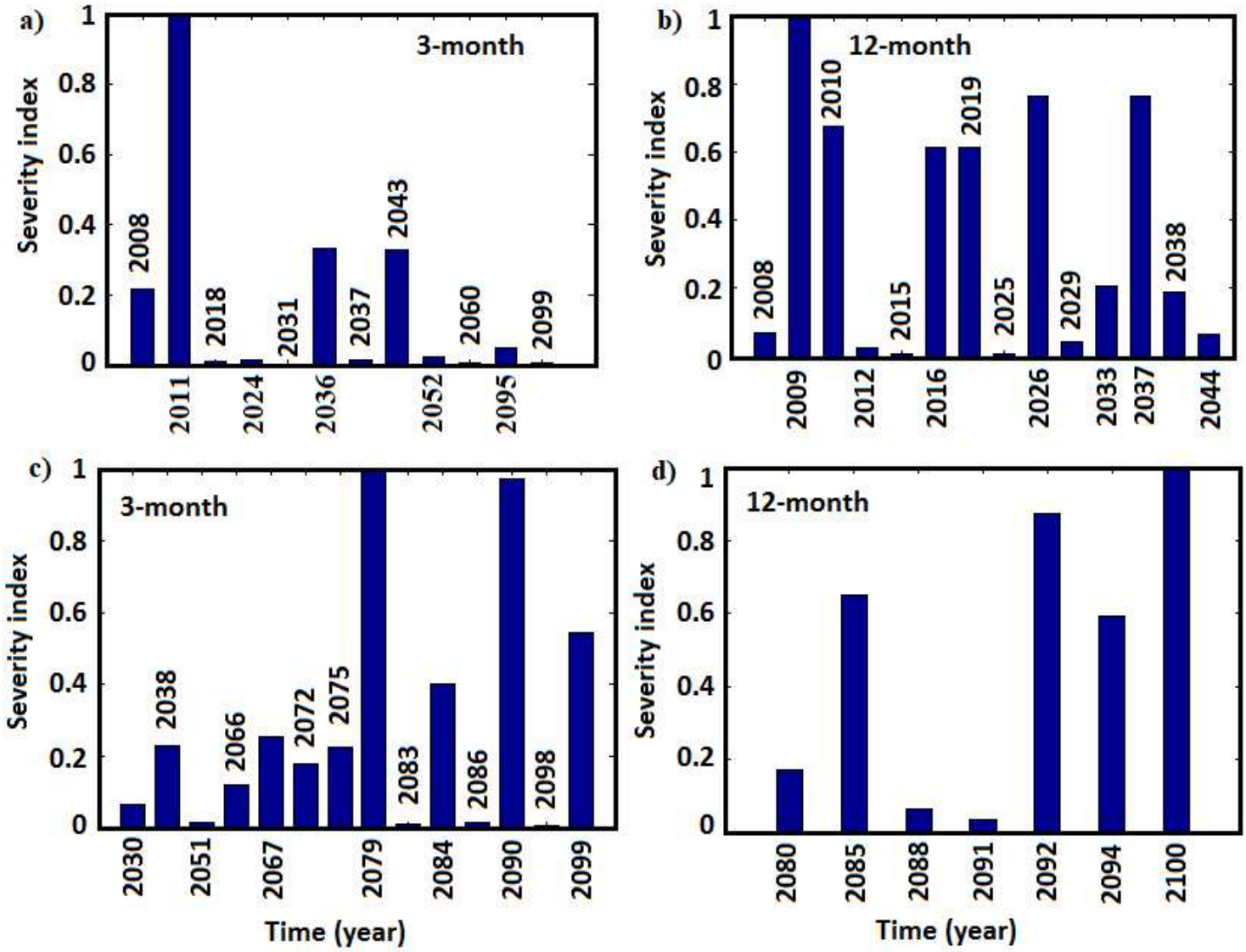

Figure 7

Assessment of severity of extreme drought years a) for at 3- month, b) for 12- month scales and extreme flood years c) for 3-month, d) for 12-month scales for 2006-2100.

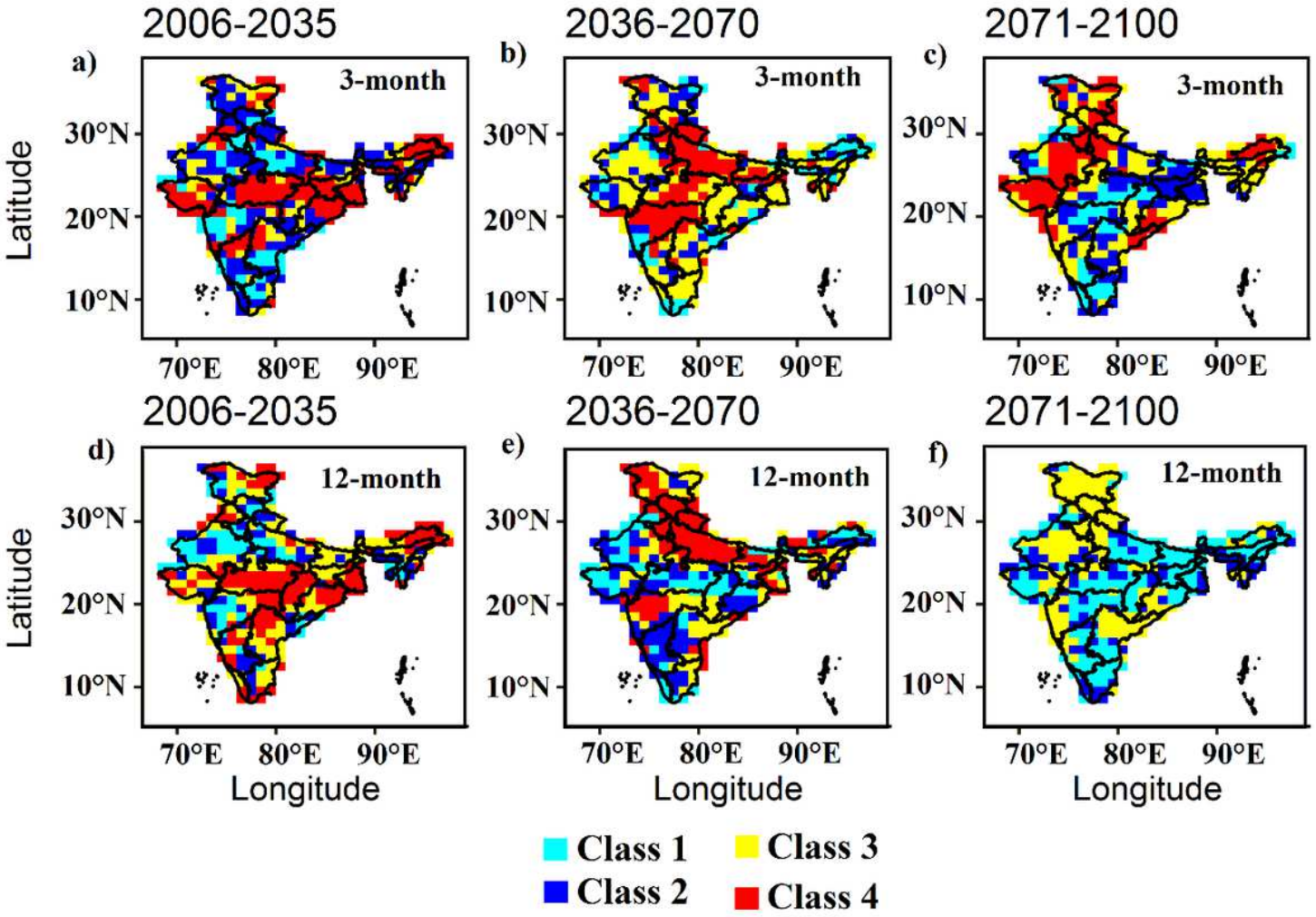

Figure 8

Spatial distribution of frequency of extreme drought years at 3- month scale for the time period: (a) 2006-2035; (b) 2036-2070; (c) 2071-2100. At 12-month scale: (d) 2006-2035; (e) 2036-2070; (f) 2071-2100.

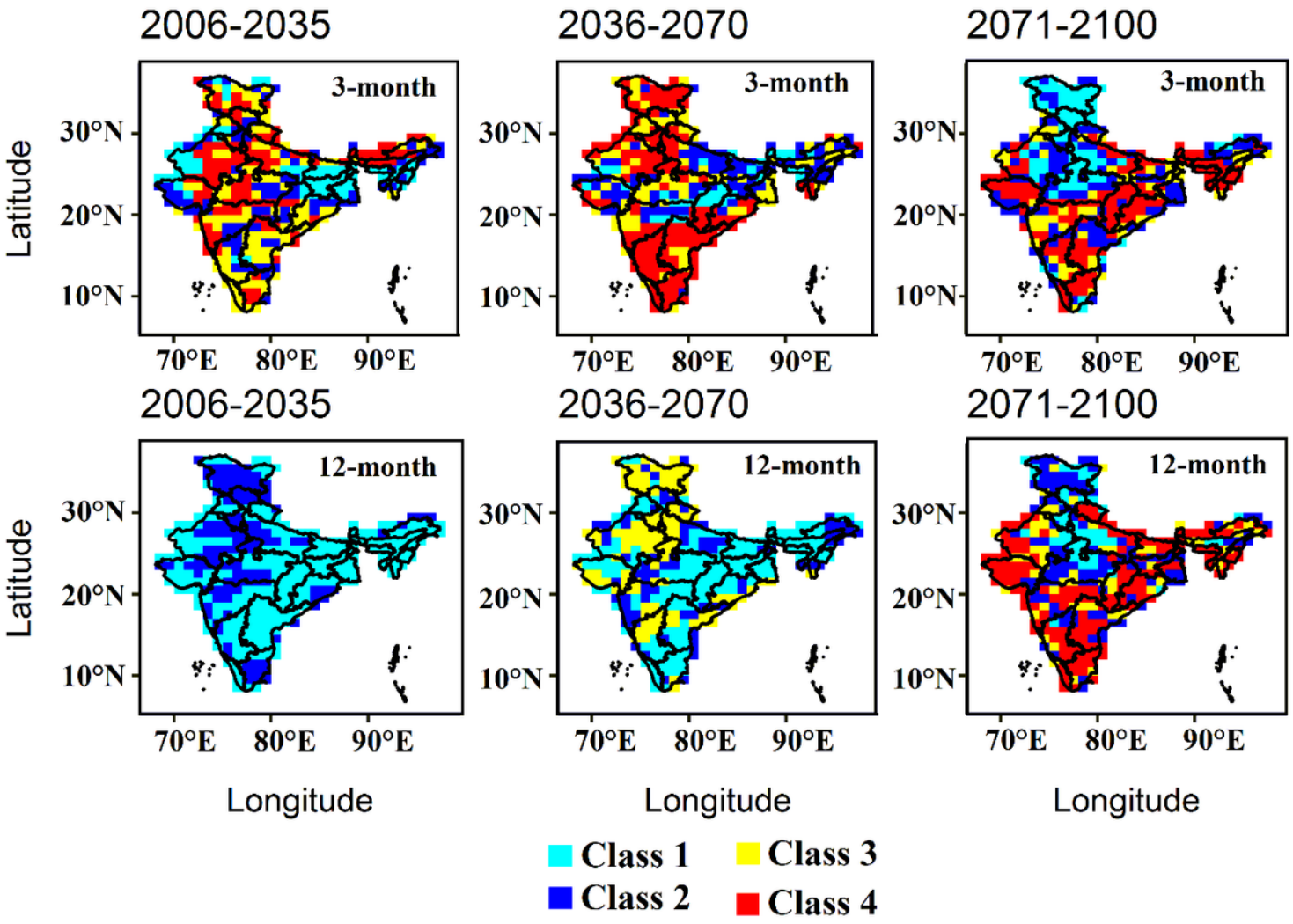

Figure 9

Spatial distribution of frequency of extreme flood years at 3- month scale for the time period a) 2006-2035; b) 2036-2070; c) 2071-2100, at 12-month scales d) 2006-2035; e) 2036-2070; f) 2071-2100.

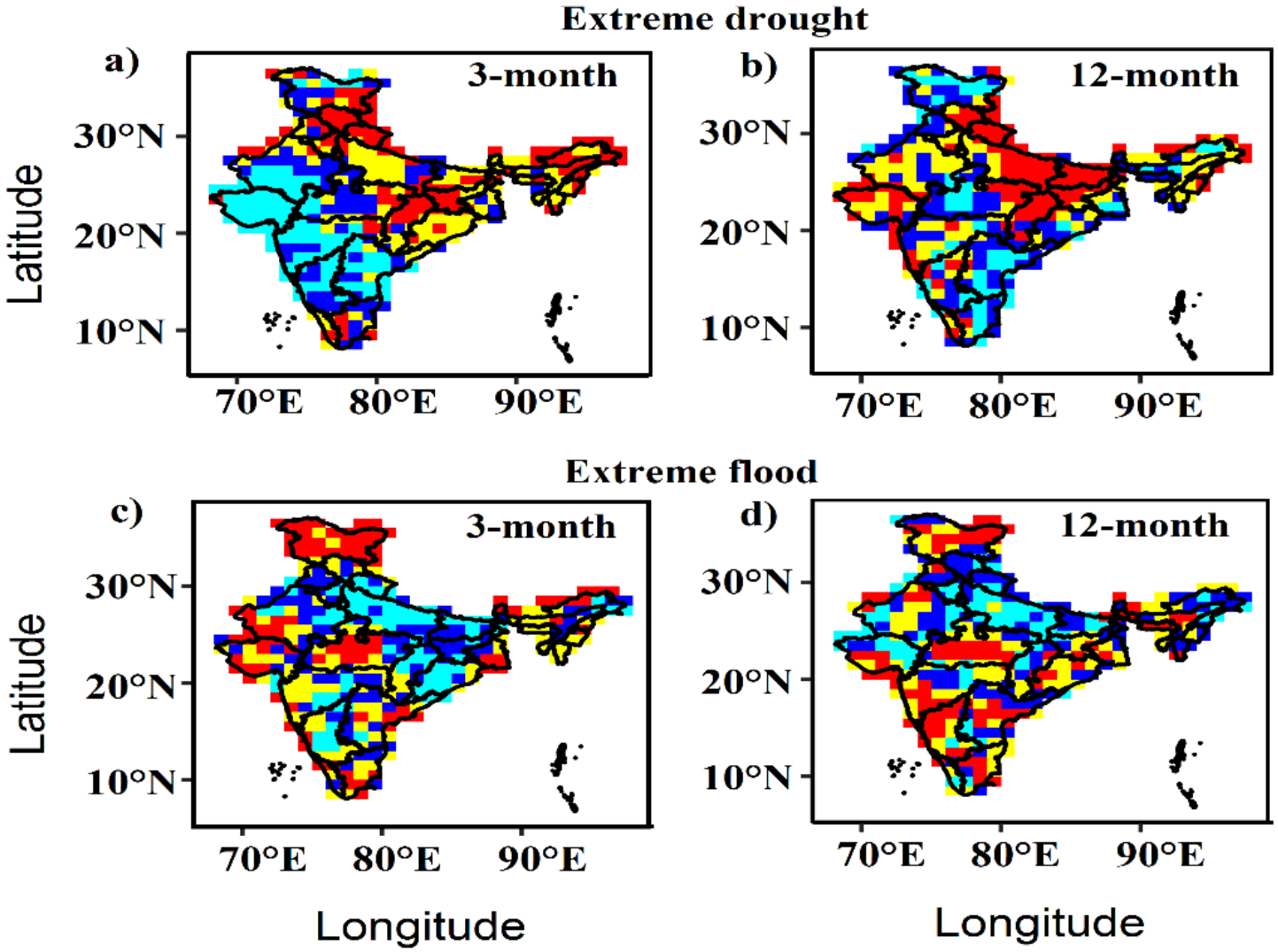

Figure 10

Classification of grids based on vulnerability index (I) of extreme drought (a) at 3- month; (b) at 12-month; and of extreme floods (c) at 3-month; (d) at 12-month scales over the period 2006-2100.